Groundwater recharge and hydrogeochemical evolution in the Ejina Basin, northwest China

Ping Wang [a], Jingjie Yu [a,*], Yichi Zhang [a], Changming Liu [a,b]

[a] *Key Laboratory of Water Cycle & Related Land Surface Processes, Institute of Geographic Sciences and Natural Resources Research, Chinese Academy of Sciences, Beijing 100101, China*
[b] *College of Resources and Environment, Beijing Normal University, Beijing 100875, China*

ARTICLE INFO

SUMMARY

Groundwater plays a dominant role in the eco-environmental protection of arid/semi-arid areas. Understanding sources and mechanisms of groundwater recharge in the Ejina Basin, an arid inland river basin in northwest China, is important for water resource planning in this ecologically sensitive area. In this study, 90 water samples were collected from rainfall, rivers and lakes, and springs and pumping wells in 2009. Analysis of the aquifer system and hydrological conditions, together with hydrogeochemical and isotope techniques were used to investigate groundwater sources and their associated recharge processes. Our results show that shallow phreatic and deep confined groundwater differ greatly in their compositions, with a distinct spatial heterogeneity of phreatic groundwater TDS (from 365 mg/L to 5833 mg/L), which increase along the shallow groundwater flow paths. Groundwater chemical evolution is mainly controlled by rock dominance and the evaporation-crystallization process, and the dominant anion species change systematically from HCO_3 to SO_4 to Cl, and the dissolved ions within the groundwater system from Na- and K-rich minerals and sulfate phases also contribute significantly to the groundwater composition. The stable isotope levels ($\delta^{18}O$ and δ^2H) of the surface water and the shallow phreatic groundwater confirm that the Heihe River and Badain Jaran Desert groundwater are the main sources recharging the phreatic aquifer in the Ejina Basin. Thus, river infiltration and desert front recharge should be considered as the two main recharge mechanisms of the Ejina aquifer. However, recharge from the Badain Jaran Desert aquifer to the Ejina Basin has occurred at a lower rate due to aridification since the middle Holocene. For this reason, the sustainable improvement of the ecological environment should be based on the shallow groundwater recharge of the phreatic aquifer in the Ejina Delta, which mainly takes place via seepage through the riverbed and direct infiltration during periods of environmental flow control.

© 2012 Elsevier B.V. All rights reserved.

1. Introduction

Desertification and rehabilitation in arid/semiarid China have been caused primarily by human activities and climatic variations, and several periods with relatively high or low rates of desertification and rehabilitation have alternated in this regions over the last thousand years (Chen et al., 2003). Areas of oases in arid inland river basins in China such as Hexi Corridor region were expected to increase as a result of high precipitation during the mid-Holocene and increased surface water diverted from rivers (Wang et al., 2008). Meanwhile, groundwater dynamics plays an important role in the eco-environmental protection of arid northwest China (Zhu et al., 2004). In the last 50 years, the increased diversion of water for irrigation from the middle reaches of the Heihe River, the second largest inland river in northwestern China, has triggered a series of ecological problems, including the disappearance of the river and terminal lakes and a severe decline of the groundwater table in its lower reaches (Feng and Cheng, 1998; Wang and Cheng, 2000; Feng et al., 2001; Chen et al., 2005; Wang et al., 2005). The decline in the groundwater table has caused large areas of vegetation die-off and has led to the ecological deterioration and desertification of the Ejina Oasis, which plays a protective role in blocking sandstorms in northwest China (Guo et al., 2009).

The ecological restoration of the Ejina Oasis should be based on the improvement of the groundwater environment, which is related to groundwater fluctuations and hydrochemistry evolution (Wang et al., 2011b), by focusing on the sources and main recharge mechanisms of the groundwater. Several studies have investigated the sources contributing to shallow and deep groundwater in the Ejina Basin. Wu et al. (2002) reported that the sources of shallow groundwater appeared to be complex and possibly included seepage from the Heihe River and local irrigation return flows, as well as the leakage of water from the confined aquifer to the phreatic aquifer. Chen

---

Table 1
Main hydrochemical characteristics and stable isotope compositions of sampled surface and groundwater in 2009.

Location	Sampling site No	Date	Z (m)	T (°C)	pH	EC (µs/cm)	Salinity (%)	TDS (mg/L)	Cl (mg/L)	SO$_4$ (mg/L)	HCO$_3$ (mg/L)	CO$_3$ (mg/L)	Na (mg/L)	K (mg/L)	Mg (mg/L)	Ca (mg/L)	Chem type	δ^{2}H (‰)	δ^{18}O (‰)
Precipitation																			
Heihe	1	12-July																−11.83	−1.29
Heihe	1	15-August																18.52	−0.44
Heihe	1	14-September																−88.13	−13.26
River water																			
Heihe	2	1-June		8.0	8.46	406	0.8	358	53.88	56.04	155.18		15.02	3.38	20.24	53.88	Ca–Mg–HCO$_3$–Cl–SO$_4$	−58.59	−10.37
Heihe	3	1-June		14.0	8.45	545	1.0	459	63.45	84.96	193.25		21.22	3.51	29.52	63.45	Ca–Mg–HCO$_3$–Cl–SO$_4$	−45.54	−7.59
Heihe	4	21-July		30.0	8.13	732	1.4	546	149.73	15.66	215.03	4.50	66.06	7.71	44.05	42.93	Mg–Na–Ca–Cl–HCO$_3$	−38.27	−4.37
Heihe	5	10-September																−34.68	−4.36
Heihe	5	1-October																−41.16	−5.32
Heihe	5	1-November																−21.52	−2.24
Lake water																			
East Juyan	6	3-June		19.2	9.44	6240	10.7	4574	1231.85	1845.26	199.10	27.25	948.00	59.03	398.10	91.58	Na–Mg–SO$_4$–Cl	2.72	2.59
East Juyan	6	10-June																3.15	2.56
East Juyan	6	20-June																13.13	6.68
East Juyan	6	1-July			9.28	7470	14.2	5603	2402.65	1241.44	118.95	33.75	1181.00	68.69	463.30	92.87	Na–Mg–Cl–SO$_4$	18.40	5.17
East Juyan	6	10-July																17.67	5.31
East Juyan	6	20-July																25.49	6.13
East Juyan	6	1-August																25.13	6.03
East Juyan	6	10-August																30.49	7.98
East Juyan	6	20-August																23.56	6.88
East Juyan	6	1-September			9.24	9527	18.1	7380	1712.98	3252.48	164.70	24.75	1614.00	91.06	610.40	99.13	Na–Mg–SO$_4$–Cl	32.16	8.50
East Juyan	6	10-September																30.73	12.74
East Juyan	6	20-September																−25.91	−3.57
East Juyan	6	1-October																−16.27	2.76
East Juyan	6	10-October																−19.87	3.32
East Juyan	6	1-November																−26.92	−1.29
East Juyan	6	1-December																−24.79	−1.69
Swan	7	31-August		21.4														41.66	12.49
Shallow phreatic groundwater (well depth < 20 m)																			
Ejina Delta	8	27-July	10	13.5	7.62	908	1.7	767	222.74	69.50	269.93		88.68	5.76	54.85	55.31	Mg–Na–Ca–Cl–HCO$_3$	−47.28	−6.94
Ejina Delta	9	27-July	<20	15.8	7.51	1065	2.0	849	242.35	89.90	274.50		103.90	5.84	60.18	72.47	Mg–Na–Ca–Cl–HCO$_3$	−47.13	−6.59
Ejina Delta	10	27-July	10	16.5	7.65	1052	2.0	854	254.35	77.33	279.08		114.10	6.15	62.25	60.52	Mg–Na–Ca–Cl–HCO$_3$	−40.28	−6.17
Ejina Delta	11	27-July	10	15.2	7.58	1138	2.1	710	256.79	113.80	233.33		194.10	15.32	38.77	26.55	Na–Mg–Cl–HCO$_3$	−51.29	−7.13
Ejina Delta	12	27-July	10	17.0	7.57	974.5	1.8	815	238.49	78.10	265.35		120.60	6.23	53.86	52.13	Na–Mg–Ca–Cl–HCO$_3$	−41.25	−6.23
Ejina Delta	13	29-August	2.91	19.0	7.49	1699	3.2	1000	174.20	456.40	269.925		186.80	8.11	72.22	83.62	Na–Mg–Ca–SO$_4$–Cl–HCO$_3$	−49.64	−6.66
Ejina Delta	14	29-August	2.38	18.6	7.45	1442	2.7	817	125.81	411.70	219.6		132.50	14.37	67.44	62.28	Na–Mg–Ca–SO$_4$–HCO$_3$	−42.27	−5.48
Ejina Delta	15	29-August	2.76	19.6	7.70	1632	3.1	973	193.56	427.30	205.875		249.30	12.22	54.42	36.43	Na–Mg–SO$_4$–Cl	−42.33	−5.59
Ejina Delta	16	29-August	15–20	17.1	7.39	1771	3.4	946	145.17	440.90	292.8		245.90	7.14	50.70	55.95	Na–Mg–SO$_4$–HCO$_3$–Cl	−68.77	−5.43
Ejina Delta	17	27-August	<15	16.8	7.47	774	1.5	664	80.65	320.70	201.3		108.80	8.90	51.97	65.96	Na–Mg–Ca–SO$_4$–HCO$_3$	−42.88	−6.08
Ejina Delta	18	29-August	15–20	14.9	8.74	612	1.2	485	87.10	214.10	150.975	6.75	127.70	7.11	30.41	18.55	Na–Mg–SO$_4$–HCO$_3$–Cl	−48.51	−3.22
Ejina Delta	19	26-July	20	14.4	7.46	6434	12.1	5833	2155.15	833.46	1120.88		977.70	18.01	483.30	244.50	Na–Mg–Cl	−44.70	−6.63
Ejina Delta	20	27-August	4.20	15.8	7.40	2956	5.6	1951	145.17	1158.00	146.4		404.00	15.95	104.60	123.70	Na–Mg–SO$_4$	−53.88	−6.54
Ejina Delta	21	31-August	<10	15.3	7.59	3497	6.6	2245	396.79	1125.00	457.5		421.30	5.81	230.70	65.80	Mg–Na–SO$_4$–Cl	−42.58	−4.78
Ejina Delta	22	31-August	5	16.6	7.52	7592	14.4	5708	1138.76	2760.00	173.85		1376.00	106.30	194.60	132.30	Na–SO$_4$–Cl	−32.86	−1.69

Table 1 (continued)

Location	Sampling site No	Date	Z (m)	T (°C)	pH	EC (µs/cm)	Salinity (%)	TDS (mg/L)	Cl (mg/L)	SO$_4$ (mg/L)	HCO$_3$ (mg/L)	CO$_3$ (mg/L)	Na (mg/L)	K (mg/L)	Mg (mg/L)	Ca (mg/L)	Chem type	δ^{2}H (‰)	δ^{18}O (‰)
Ejina Delta	23	25-July	7	15.0	7.59	4395	8.3	3487	1214.58	606.97	512.40		652.10	62.27	270.10	168.80	Na–Mg–Cl–SO$_4$	−40.91	−5.96
Gurinai	24	21-July	2.30	17.0	7.44	1219	2.3	707	238.60	163.12	237.90		218.40	8.71	22.97	40.19	Na–Cl–HCO$_3$–SO$_4$	−74.36	−9.01
Gurinai	25	21-July	3.15	17.5	7.67	2174	4.2	1153	355.64	217.41	530.70		530.40	23.03	8.82	17.56	Na–Cl–HCO$_3$	−50.50	−2.48
Gurinai	26	21-July	2.45	14.0	7.65	904.2	1.7	476	145.02	95.30	192.15		167.90	10.07	16.83	23.57	Na–Cl–HCO$_3$–SO$_4$	−40.04	−0.83
Gurinai	27	21-July	4.60	17.6	7.66	892.9	1.7	432	74.58	134.56	256.20	4.50	181.80	10.50	11.15	19.51	Na–HCO$_3$–SO$_4$–Cl	−47.06	−1.30
Gurinai	28	21-July	2.32	12.5	7.75	721.4	1.3	365	122.04	62.14	169.28		150.20	7.87	8.76	12.37	Na–Cl–HCO$_3$	−54.01	−2.90
Gurinai	29	21-July	2.30	15.8	7.58	1284	2.4	686	157.10	225.12	269.93		225.00	14.24	30.01	34.14	Na–SO$_4$–Cl–HCO$_3$	−51.60	0.68
Gurinai	30	20-July	9.00	15.0	7.67	1315	2.5	753	221.06	232.49	219.60		222.40	17.00	33.48	26.87	Na–Cl–SO4–HCO$_3$	−40.11	2.49
Gurinai	31	20-July	3.10	15.0	7.43	2108	4.0	1261	319.81	417.05	210.45		394.80	56.86	29.46	42.55	Na–Cl–SO$_4$	−36.73	0.39
Gurinai	32	20-July	2.70	18.0	7.38	2347	4.4	1399	288.70	466.33	603.90		453.00	41.47	66.52	82.63	Na–HCO$_3$–SO$_4$–Cl	−40.98	−0.14
Gurinai	33	20-July	1.80	18.5	7.55	4315	8.2	2662	496.39	1140.58	411.75		830.00	32.66	75.09	87.28	Na–SO$_4$–Cl	−55.81	−6.16
Gurinai	34	20-July	2.00	17.5	7.50	3732	7.1	2590	986.22	591.87	324.83		641.00	25.71	115.00	126.60	Na–Mg–Cl–SO$_4$	−71.38	−8.56
Guanzihu	35	25-August	2.25	15.5	7.65	802.3	1.5	409	106.46	132.70	137.25		138.50	6.21	9.44	15.33	Na–Cl–SO$_4$–HCO$_3$	−50.15	−1.93
Guanzihu	36	25-August	3.00	19.2	7.06	1006	1.9	530	170.98	143.50	150.975		136.60	13.48	22.69	30.77	Na–Cl–SO$_4$–HCO$_3$	−45.96	−1.26
Guanzihu	37	25-August	<5	12.6	7.83	800	1.5	417	135.49	121.30	91.5		102.00	13.59	19.63	20.91	Na–Mg–Cl–SO$_4$	−48.75	−1.65
Guanzihu	38	25-August	4.05	18.6	7.17	1061	2.0	564	164.52	155.40	137.25		114.70	18.65	27.67	44.90	Na–Mg–Ca–Cl–SO$_4$–HCO$_3$	−45.47	−1.61
Guanzihu	39	25-August	3.48	12.7	7.71	1104	2.1	571	196.78	134.80	123.525		164.70	10.71	20.52	30.65	Na–Cl–SO$_4$	−51.98	−2.13
Guanzihu	40	25-August	3.00	19.0	7.20	1065	2.0	514	161.30	143.90	128.1		153.90	11.53	17.43	26.21	Na–Mg–SO$_4$–HCO$_3$	−49.90	−0.33
Guanzihu	41	25-August	3.70	16.1	7.38	2038	3.9	1072	277.43	254.75	420.9		276.00	22.58	59.73	77.23	Na–Mg–Cl–HCO$_3$–SO$_4$	−58.50	−3.35
Guanzihu	42	25-August	2.40	16.4	7.92	2120	4.0	1173	477.44	220.40	347.7		388.20	17.13	24.40	44.92	Na–Cl–HCO$_3$–SO$_4$	−65.95	−5.17
Guanzihu	43	25-August	2.30	20.1	7.37	3356	6.4	1934	625.83	564.10	228.75		570.90	20.32	38.00	115.20	Na–Cl–SO$_4$	−61.51	−4.34
Guanzihu	44	25-August	<5	17.4	7.30	5197	9.8	3237	1009.72	1097.39	114.375		795.60	17.99	100.50	216.10	Na–Ca–Cl–SO$_4$	−73.64	−8.17

Middle phreatic/confined groundwater (well depth = 20–100 m)

Location	Sampling site No	Date	Z (m)	T (°C)	pH	EC (µs/cm)	Salinity (%)	TDS (mg/L)	Cl (mg/L)	SO$_4$ (mg/L)	HCO$_3$ (mg/L)	CO$_3$ (mg/L)	Na (mg/L)	K (mg/L)	Mg (mg/L)	Ca (mg/L)	Chem type	δ^{2}H (‰)	δ^{18}O (‰)
Ejina Delta	45	31-August	40–50	16.7	7.23	4354	8.3	3082	512.93	1574.00	498.675		567.80	11.86	265.80	149.40	Na–Mg–SO$_4$–Cl	−44.52	−2.41
Ejina Delta	46	28-August	40–50	11.5	7.30	3274	6.2	2096	493.57	891.63	388.875		463.80	8.02	165.00	74.32	Na–Mg–SO$_4$–Cl	−42.20	−4.90
Ejina Delta	47	25-July	80	12.0	7.65	3968	7.5	2945	1091.44	745.32	192.15		510.00	16.36	224.60	165.10	Na–Mg–Cl–SO$_4$	−47.88	−6.15
Ejina Delta	48	25-July	80	14.3	7.71	3653	6.9	2836	927.86	492.21	521.55		521.20	17.25	226.90	128.90	Na–Mg–Cl–SO$_4$	−46.42	−6.37

Deep confined groundwater (well depth > 100 m)

Location	Sampling site No	Date	Z (m)	T (°C)	pH	EC (µs/cm)	Salinity (%)	TDS (mg/L)	Cl (mg/L)	SO$_4$ (mg/L)	HCO$_3$ (mg/L)	CO$_3$ (mg/L)	Na (mg/L)	K (mg/L)	Mg (mg/L)	Ca (mg/L)	Chem type	δ^{2}H (‰)	δ^{18}O (‰)
Ejina Delta	49	27-July	130	13.0	7.58	894.6	1.7	737	214.05	59.20	256.20		84.27	6.46	59.15	57.66	Mg–Na–Ca–Cl–HCO$_3$	−46.64	−7.72
Ejina Delta	50	29-August	>100	19.6	8.77	1298	2.5	629	170.98	205.76	91.5	11.25	205.10	7.19	27.45	12.43	Na–Cl–SO$_4$	−71.82	−9.20
Ejina Delta	51	27-August	180	15.0	8.30	1089	2.1	546	119.36	197.10	187.575		210.70	1.30	7.99	9.81	Na–SO$_4$–Cl–HCO$_3$	−57.09	−7.80
Ejina Delta	52	25-July	140	12.5	7.99	915.5	1.7	537	172.44	106.00	205.88		152.50	2.14	25.54	32.52	Na–Mg–Cl–HCO$_3$–SO$_4$	−51.56	−8.06
Ejina Delta	53	27-August	>100	14.0	9.29	2732	5.2	1479	409.70	485.62	114.375	24.75	557.70	8.85	12.30	4.88	Na–Cl–SO$_4$	−60.07	−7.83
Ejina Delta	54	27-August	>100	22.6	7.29	1714	3.3	1014	225.82	431.12	109.8		242.30	1.00	20.37	93.68	Na–Ca–SO$_4$–Cl	−86.84	−9.64
Ejina Delta	55	27-August	>100	15.0	7.39	1862	3.5	1162	225.82	538.90	109.8		241.20	1.24	29.65	125.40	Na–Ca–SO$_4$–Cl	−84.04	−5.70
Gurinai	56	20-July	144	19.0	7.76	882.1	1.7	462	124.58	128.43	155.55	4.50	173.40	13.77	11.75	10.50	Na–Cl–SO$_4$–HCO$_3$	−57.00	−3.61

Spring

| Location	Sampling site No	Date	Z (m)	T (°C)	pH	EC (µs/cm)	Salinity (%)	TDS (mg/L)	Cl (mg/L)	SO$_4$ (mg/L)	HCO$_3$ (mg/L)	CO$_3$ (mg/L)	Na (mg/L)	K (mg/L)	Mg (mg/L)	Ca (mg/L)	Chem type	δ^{2}H (‰)	δ^{18}O (‰)
Ejina Delta	57	1-September																−57.11	−8.47
Ejina Delta	57	1-November																−57.37	−4.63
Ejina Delta	58	3-June																−52.97	−7.09
Ejina Delta	58	1-July			8.28	2679	5.1	1705	581.60	486.77	128.10		479.20	2.49	27.81	127.40	Na–Ca–Cl–SO$_4$	−76.18	−9.75
Ejina Delta	58	1-August																−81.69	−9.53
Ejina Delta	58	1-September			7.55	2451	4.7	1555	425.83	558.49	109.80		434.00	1.57	24.54	110.40	Na–Ca–Cl–SO$_4$	−83.50	−8.88
Ejina Delta	58	1-October																−80.16	−9.60
Ejina Delta	58	1-November																−83.08	−9.95
Ejina Delta	58	1-December																−83.95	−9.50
Gurinai	59	21-July		13.7	7.54	625.2	1.2	301	77.82	58.01	192.15		117.50	8.04	9.30	17.52	Na–HCO$_3$–Cl	−43.56	−1.28
Gurinai	60	21-July		15.8	7.59	622.16	1.2	296	87.43	56.92	164.70		134.50	5.44	5.36	6.54	Na–HCO$_3$–Cl	−47.92	1.90
Guanzihu	61	25-August		12.9	7.10	830	1.6	423	135.49	119.80	100.65		105.50	14.25	20.28	20.96	Na–Mg–Cl–SO$_4$–HCO$_3$	−44.65	−1.28
Guanzihu	62	25-August		14.3	7.51	887.6	1.6	393	116.13	121.30	91.5		99.59	12.28	19.68	20.38	Na–Mg–Cl–SO$_4$–HCO$_3$	−46.21	−1.62
Guanzihu	63	25-August		12.7	7.47	1395	2.6	736	245.17	208.40	118.95		195.70	7.64	22.64	52.28	Na–Cl–SO$_4$	−71.89	−1.87
Guanzihu	64	25-August		11.7	7.01	1152	2.2	580	38.71	304.64	183		164.60	8.20	20.79	43.24	Na–SO$_4$–HCO$_3$	−73.30	−5.51
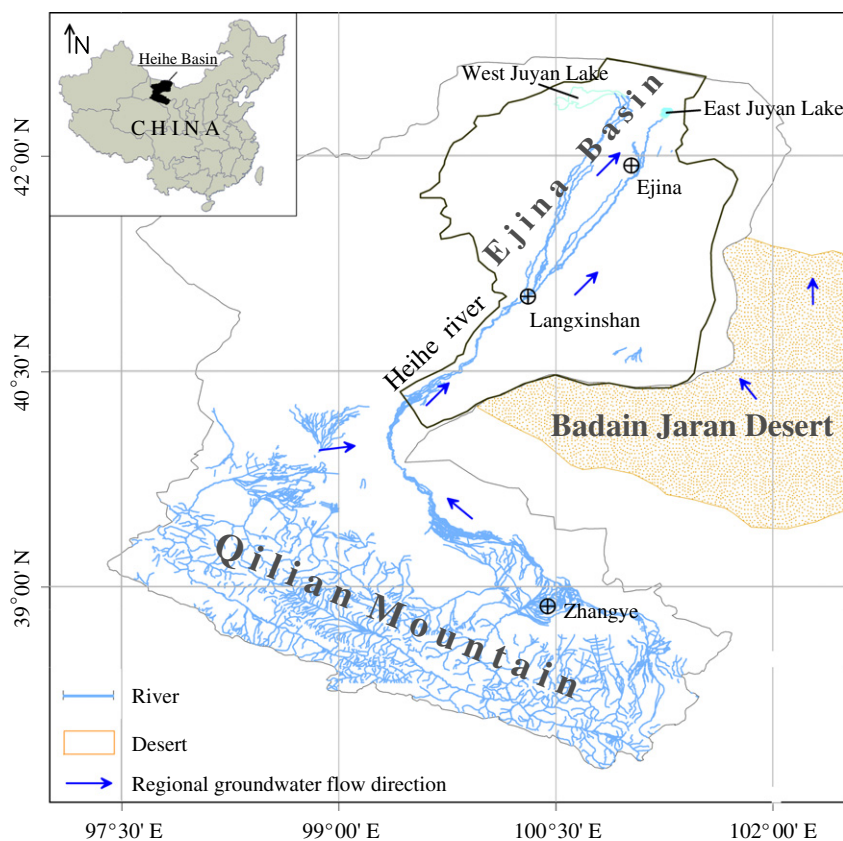
Fig. 1. Map of the Ejina Basin showing its relationship to the Heihe Basin and the Badain Jaran Desert.

et al. (2006) concluded that direct recharge from the Heihe River was the primary source of the shallow groundwater and that the mean residence time of groundwater recharge was 26 years in the Ejina Oasis. Based on data from experimental observations, Xi et al. (2010a) supported this conclusion using a simulation analysis of spatial and temporal variations in the groundwater level and the regional hydrologic regime in a recent 10-year period in the Ejina region. In addition, field observations indicated that shallow groundwater in the western and northern bordering range of the Badain Jaran Desert was recharged by desert groundwater (Yang et al., 2003; Yang and Williams, 2003). Moreover, Gates et al. (2008) also proposed that Gurinai is most likely a discharge zone for the Badain Jaran shallow aquifer based on regional hydraulic head patterns. This suggested that groundwater from the Badain Jaran Desert could be another source of shallow groundwater recharge in the Ejina Basin. Qian et al. (2006) investigated the recharge sources of deep groundwater and its circulation in the Ejina Basin, and their study assumed that the deep groundwater in the riparian area was mainly recharged by the Heihe River water, while the deep groundwater recharge in the Gurinai area was dominated by lateral groundwater inflow from the Badain Jaran Desert. Based on the isotope analyses of groundwater (^{3}H and ^{14}C) in the Ejina Basin, Chen et al. (2004b) indicated that the groundwater age in confined aquifers was more than 2000 a, and the deep confined groundwater in the north area was mainly recharged by the groundwater from the north Mongolia plateau (Qian et al., 2006). In addition, Chen et al. (2004a) proposed that there was rapid transfer of snow melt from the Qilian Mountains through fracture networks to the Badain Jaran Desert, which then flowed to the Ejina Basin.

Recent work has documented the shallow groundwater recharge characteristics in the study area using hydrochemistry and isotopic techniques. For instance, Feng et al. (2004) investigated the distribution and evolution of water chemistry in the Heihe River Basin and concluded that since the 1960s, the large volumes of the river water diverted for irrigation have re-emerged as springs at the edge of alluvial fans and then flowed into the Heihe River. Wen et al. (2005) investigated the hydrochemical characteristics and salinity of groundwater in the Ejina Basin. Their results indicated that within 1 km of the river water influence zone, the groundwater was recharged directly from the Heihe River, and from 1 km to 10 km of the river water influence zone, the groundwater source was a mixture of different waters. Si et al. (2009) conducted a hydrochemical survey and demonstrated the complexity of the hydrochemical components of groundwater in the Ejina Basin, where exhibited a clear zonation from the recharge area to the discharge area.

However, both the surface water resources in the Heihe River and the groundwater resources in the Badain Jaran Desert have been significantly affected by climate change (e.g. Yang et al., 2003, 2010; Zhang et al., 2007). In addition, the implementation of environmental flow controls (the allocation of a certain amount of water to the lower reaches of the Heihe River to protect the Ejina Oasis from deterioration) in the Heihe River since 2000 have had an impact on the surface and groundwater regime in the Ejina Basin (Wang et al., 2011a). Therefore, although remarkable advances have been made in water resources research over the past decade, the infiltration-recharge mechanisms and the hydrochemical evolution of groundwater in the study area are still not well understood, especially considering the combined effects of climate change and human activities. The objective of this study is to establish mechanisms of recharge associated with hydrogeochemical evolution for the shallow Quaternary aquifer of the Ejina Basin using environmental tracers, including ion chemistry and stable isotopes of water.
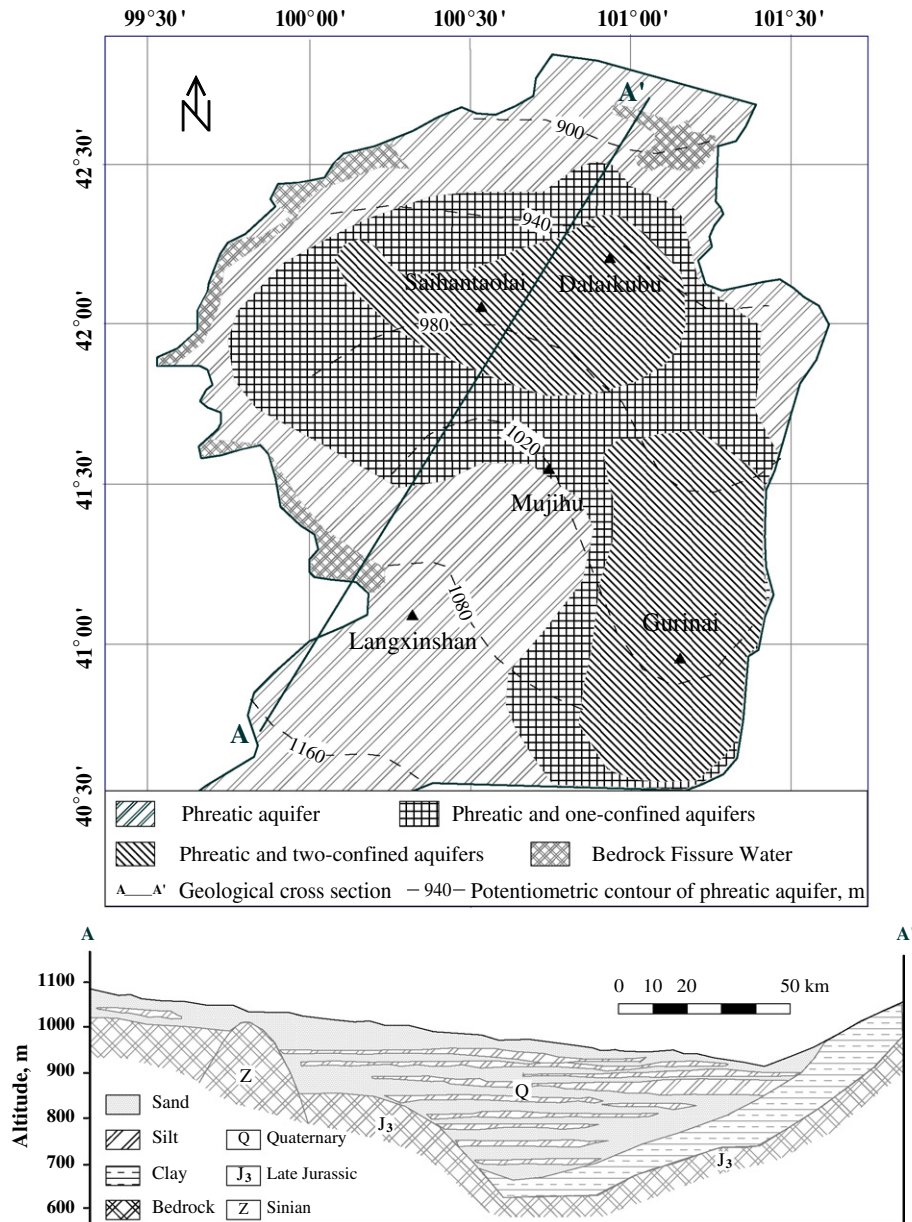
Fig. 2. Hydrogeologic units and geological cross-section of the Ejina Basin (modified from Wu et al., 2002 and Xi et al., 2010a). Q, J3 and Z are the geologic periods.

2. The study area

The Ejina Basin covers an area of 3×10^4 km^2 in northwest China, extending between latitudes of 40°20′–42°30′N and longitudes of 99°30′–102°00′E (Fig. 1). This region is characterized by a continental climate that is extremely hot in the summer and severely cold in the winter. The mean annual temperature is approximately 8 °C, with a maximum daily temperature of 41 °C (July) and a minimum of −36 °C (January). According to observational data from 1957 to 2005 at the Ejina weather station, the mean annual precipitation is only 42 mm, and the mean annual pan evaporation (20 cm in diameter and 11 cm in depth) is 3755 mm (Xi et al., 2010b). The topography of the basin inclines from the southwest to the northeast with an average slope of 1–3‰, and the surface elevation varies from 1127 m to 820 m above sea level (Akiyama et al., 2007). The dominant landscape of the Ejina Basin is that of the Gobi Desert, which is composed of wind-eroded hilly areas, desert, and alkaline soils (Xie, 1980; Feng et al., 2004; Akiyama et al., 2007). The natural

vegetation that exists in the region is distributed along the rivers and relies on shallow groundwater for sustenance (Xie, 1980; Feng et al., 2004; Akiyama et al., 2007).

The Heihe River, originating in Qilian Mountain, is the main recharge source of the groundwater system, and approximately 66% of the groundwater recharge in the Ejina alluvial fan occurs through vertical percolation from the Heihe River (Wu et al., 2002). The Heihe River flows through the Ejina Basin and divides into two branches at Langxinshan (Fig. 1). The two branches of the Heihe River flow to the East and West Juyan Lakes; the total length of the two branches in the basin is approximately 240 km. The riverbed is wide and shallow, consisting of coarse sand and gravel with high permeability (Xie, 1980; Si et al., 2009). The main mechanisms of groundwater discharge are evaporation, transpiration and groundwater extraction (Xie, 1980; Feng et al., 2004; Wen et al., 2005; Si et al., 2009; Xi et al., 2010b).

The study area represents a regional geotectonic basin, and the eastern edge of the basin is bounded by the hidden Badain Jaran
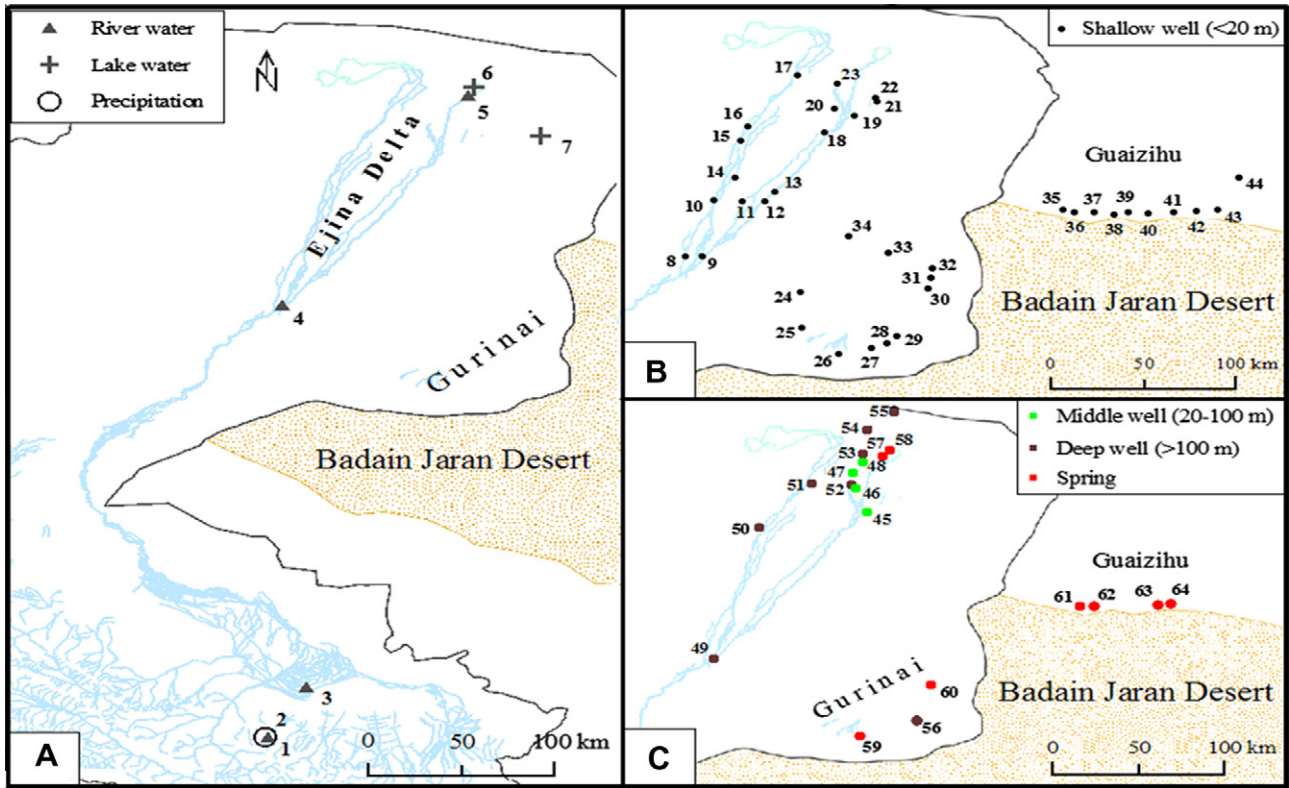
Fig. 3. Map of water sample locations: A – surface water and precipitation; B – shallow groundwater; C – middle and deep groundwater and spring water.
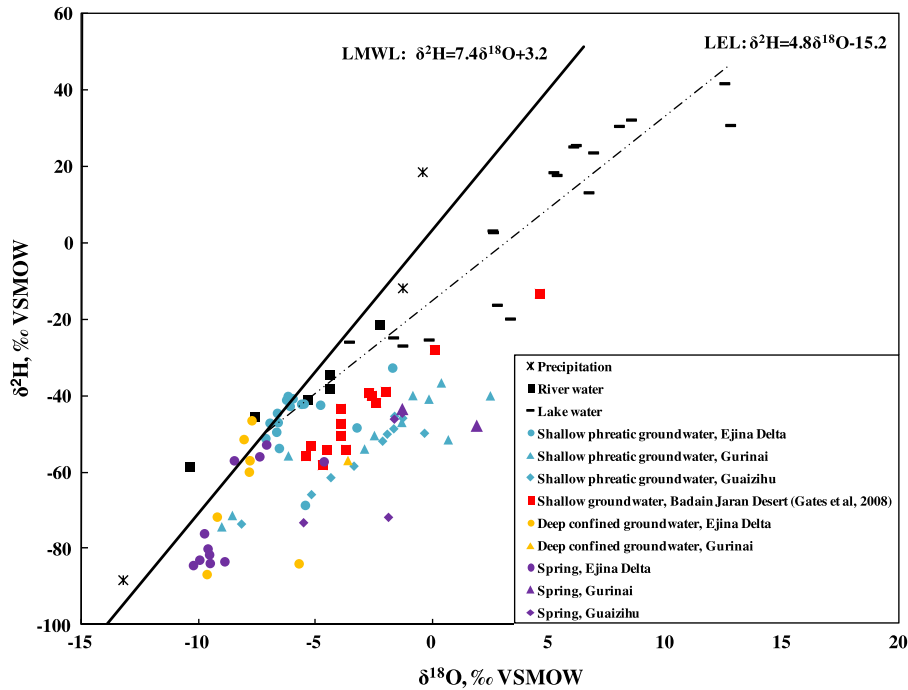

Fig. 4. $\delta^{18}O–\delta^2H$ diagram of the surface and ground waters.

Desert Fault. The southern edge of the basin lies along the fault of the Alashan uplift, and the northern and western edges lie along the bedrock of adjacent mountains (Xie, 1980; Wu et al., 2002; Wen et al., 2005). The bedrock of the Ejina Basin is composed of Sinian (Z) and Late Jurassic (J₃) formations, and the basin is filled with unconsolidated Quaternary (Q) sediments with a depth of several hundred meters (Fig. 2) that form an independent aquifer system (Xie, 1980; Wu et al., 2002). The regional Quaternary aquifers vary from a zone of unconfined gravel and pebbles to a multi-layered zone that consists of sand and silt (Xie, 1980). The Langxinshan–Mujihu uplift controls the distribution of Quaternary sediments and divides the Basin into two depositional depressions:
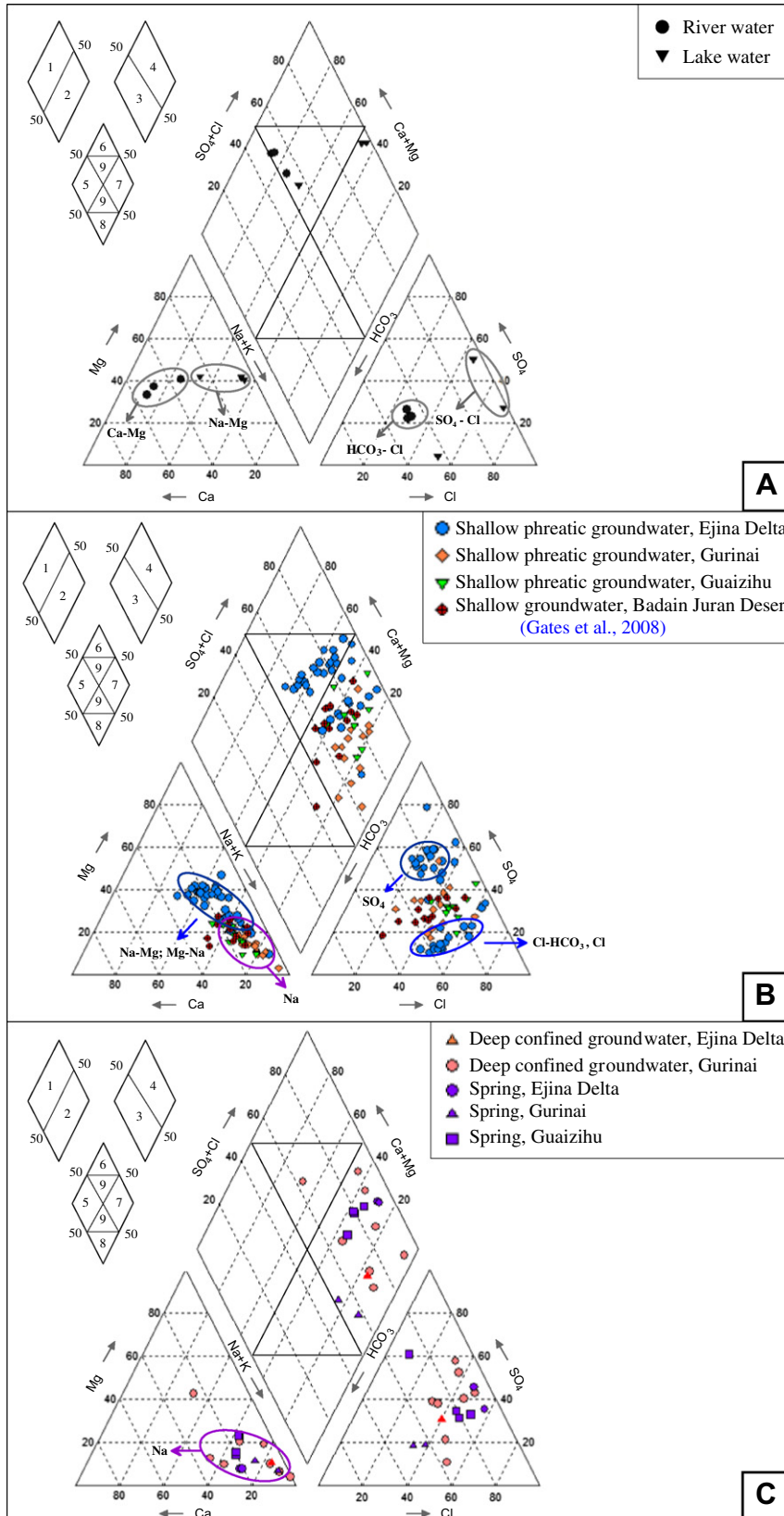
Fig. 5. Piper diagram of sampled surface water and groundwater: A – surface water; B – shallow phreatic groundwater; C – deep confined groundwater and spring water (zone 1: alkaline earths (Ca + Mg) exceed alkalis (Na + K); zone 2: alkalis exceed alkaline earths; zone 3: weak acids (CO$_3$ + HCO$_3$) exceed strong acids (SO$_4$ + Cl); zone 4: strong acids exceed weak acids; zone 5: carbonate hardness >50% (alkaline earths and weak acid dominate); zone 6: non-carbonate hardness >50%; zone 7: non-carbonate alkali >50%; zone 8: carbonate alkali >50% (groundwater is inordinately soft in proportion to the content of TDS); zone 9: no cation–anion pair >50% (Piper, 1944)).
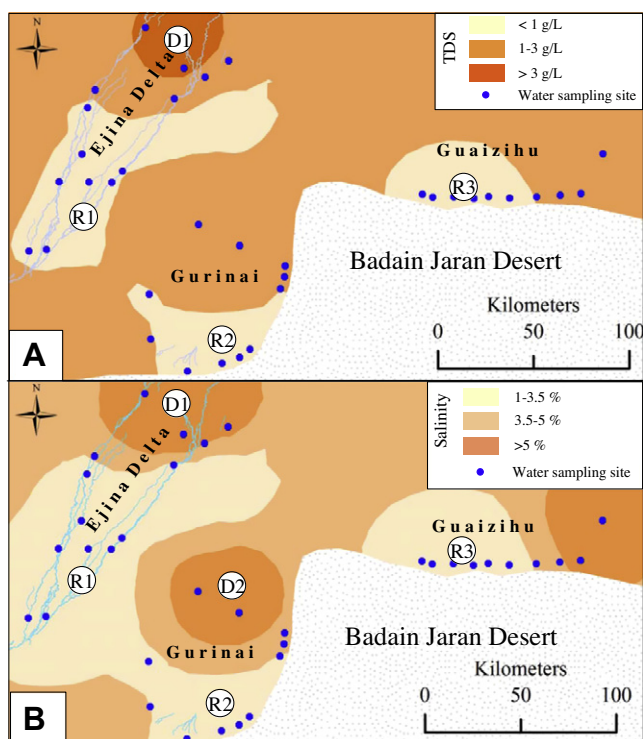
Fig. 6. Spatial variation of the TDS (g/L) and salinity (%) of shallow phreatic groundwater (R1, R2, R3 – recharge zones; D1, D2 – discharge zones).

the Saihantaolai-Dalaikubu Depression in the northwest and the Gurinai Depression in the southeast (Fig. 2). The depositional construction and a variety of lithofacies control the distribution characteristics of aquifer systems. From the south to the north of the basin, the lithologic features of the aquifer system gradually vary from gravel to fine sand (Wen et al., 2005). In general, shallow groundwater flows from the south to the northeast across the basin. The phreatic aquifer in the southern part of the basin is recharged by river water, and the groundwater separates into two flow directions: towards the Juyan Lakes and towards Gurinai (Xie, 1980; Wen et al., 2005; Si et al., 2009).

In the Ejina Basin, the predominant vegetation, which is characterized by species such as *Populus euphratica*, *Tamarix ramosissiman*, and *Sophora alopecuroides*, mainly depends on groundwater for sustenance (Zhu et al., 2009). In recent decades, over-extraction of the groundwater has caused a decline in the water table, resulting in the shrinking of large areas of *P. euphratica*, thus creating a highly visible indicator of ecological change and desertification in the Ejina Basin (Guo et al., 2009). Therefore, to determine the groundwater recharge sources for the Ejina Basin and the contribution of these sources to shallow phreatic groundwater is essential for water resource planning in this ecologically sensitive area.

3. Materials and methods

Water samples were collected during the period from June to December 2009 from 64 sites along the Heihe River, as well as within the Ejina Delta and areas of Gurinai (western margin of the Badain Jaran Desert) and Guaizihu (northern margin of the Badain Jaran Desert) (Fig. 3), including three precipitation samples, 23 surface water samples (6 river water and 17 lake water samples) and 64 groundwater samples. Rainfall samples were collected in the upper reaches of the Heihe Basin at the foot of the Qilian Mountain (sampling site No. 1 in Fig. 3A). Surface water samples were obtained from the Heihe River at four sites (sampling sites No. 2–5 in Fig. 3A) representing the upper, middle and lower reaches of the river, as well as from East Juyan Lake (sampling site No. 6 in Fig. 3A) and Swan Lake (sampling site No. 7 in Fig. 3A). Surface water was sampled by submerging sample bottles to a depth of some 5 cm below the water surface, and lake water samples were obtained in the centre of the lakes.

To the extent possible, groundwater samples were from regularly used pumped wells or boreholes and springs to ensure that samples were as representative as possible of in situ conditions. Samples of shallow groundwater were typically collected from wells <20 m deep (long-term observation wells and wells used for domestic purpose) but were also collected at depths up to 100 m (irrigation wells), and samples of deep groundwater (>100 m) were primarily obtained from industrial wells. Considering the hydrogeological conditions in the study area, particularly the hydraulic characteristics of the aquifer systems and the potential impact of surface/groundwater interaction on groundwater dynamics, the groundwater samples were grouped into the following categories: shallow groundwater (<20 m, phreatic aquifer); middle groundwater (20–100 m, phreatic or confined aquifer), deep groundwater (>100 m, confined aquifer) and spring water.

Major ions and stable isotopes ($\delta^{18}O$ and δ^2H) of the sampled water were analyzed at the Centre Laboratory for Physical and Chemical Analysis, Institute of Geography Sciences and Natural Resources Research, Chinese Academy of Sciences in Beijing. SO_4 and Cl were analyzed using an ion chromatograph (IC), and HCO_3 (CO_3) anions were analyzed by titration (0.01 N H_2SO_4). Cations were analyzed using an inductively coupled plasma (ICP-MS) method. All water chemistry results were within a 5% ionic charge balance. Stable isotopes of water ($\delta^{18}O$ and δ^2H) were determined by isotope ratio mass spectrometry using Finnigan MAT 253 after online pyrolysis with a Thermo Finnigan High Temperature Conversion Elemental Analyzer (TC/EA) (http://www.thermoscientific.com) and reported relative to the VSMOW standard (*Vienna Standard Mean Ocean Water*) in per mille ($\delta‰$).

In addition to the major ion water chemistry, the water temperature (T), pH, electrical conductivity (EC) and total salinity were used as the main indicators in our analysis and evaluation of the water chemistry and its spatiotemporal evolution. These parameters were measured in situ using a HANNA HI 98188 Waterproof, Portable EC/Resistivity/TDS/NaCl and Temperature Meter, and CyberScan PC300 Waterproof Portable pH/ORP/Conductivity Meters.

4. Results

Hydrochemical results (site information, field data and major ions) and the stable isotope compositions of the surface water and groundwater are presented in Table 1 and the sample locations in Fig. 3. The water samples from the Heihe River were obtained from four sites (sampling sites No. 2–5) representing the upper, middle and lower reaches of the river (Fig. 1). The river water was slightly alkaline, with a mean pH value of 8.13–8.46, and it was fresh water, being characterized by salinities from 0.8% to 1.4%. Generally, the river water salinity increased along river flow paths, indicating the occurrence of evaporation. The sampled surface waters from the lakes exhibited pH values in excess of 9.0 (9.24–9.44) and high salinity (from 10.7% to 18.1%) due to significant evaporative concentration. The lake waters tended to be dominated by Mg and Na cations and SO_4 and Cl anions (Table 1).

According to the investigations conducted in July–August 2009, the groundwater temperature ranged from 11.5 °C (sampling site No. 46) to 22.6 °C (sampling site No. 54). The mean temperature of the shallow phreatic groundwater (16.4 °C) was higher than the middle phreatic/confined groundwater (13.6 °C) and spring water (13.5 °C). The pH, which was one of the primary indicators
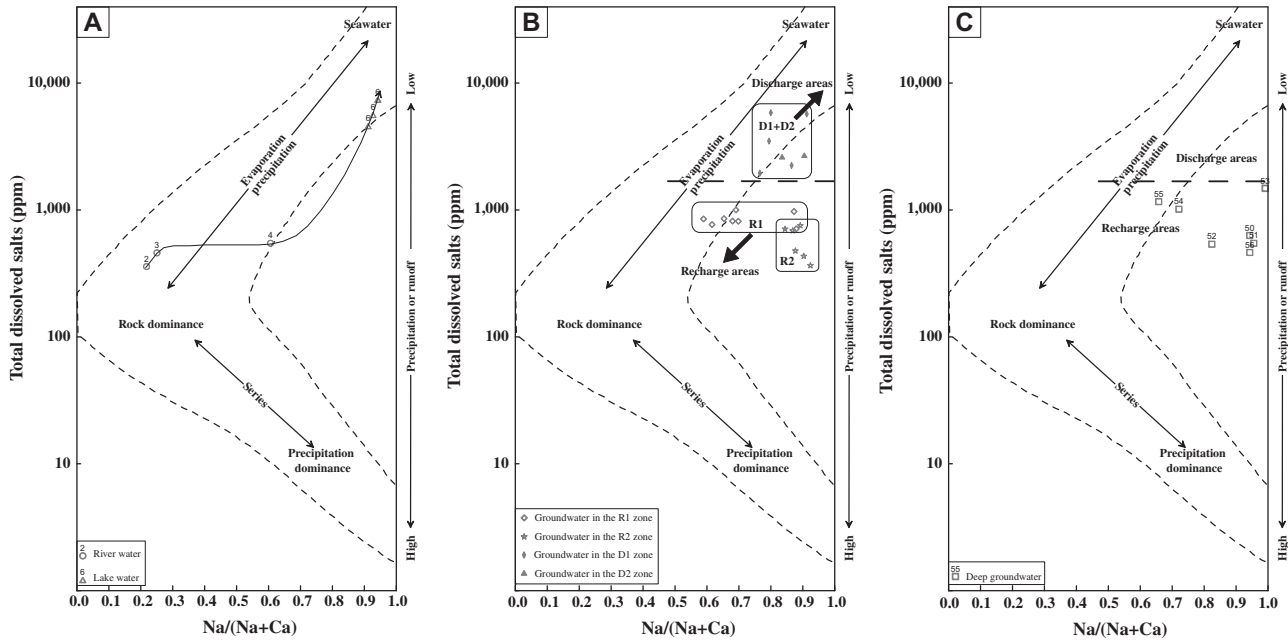
Fig. 7. Diagrammatic representation of processes controlling the chemistry of nature waters: A – surface water; B – shallow phreatic groundwater; C – deep confined groundwater.

of the water chemistry evolution, generally ranged from 7.01 to 9.29, indicating a neutral to slightly alkaline character. The slightly alkaline character of the groundwater resulted from the extremely dry conditions and the slow groundwater flow characteristics in the study area. The groundwater samples were characterized by a high degree of variability with respect to TDS (the total dissolved solids), which ranged from 365 mg/L (sampling site No. 28) to 5833 mg/L (sampling site No. 19), indicating that the quality of the groundwater varied greatly, ranging from fresh to saline. The highest groundwater EC values (2956–7592 μs/cm) were observed in the Saihantaolai-Dalaikubu Depression, indicating the influence of the aquitard below (Feng et al., 2004).

Fig. 4 shows the relationship between δ^2H and δ^{18}O for both surface and groundwater. The stable isotope data for precipitation and river water exhibited a range from −88.1‰ to +18.5‰ for δ^2H and −13.3‰ to −0.4‰ for δ^{18}O. The lake water samples tended to be heavier than the surface water in δ^2H (−26.9 to +41.7‰) and δ^{18}O (−3.6 to +12.5‰) due to evaporative enrichment. The stable isotope values of the groundwater ranged from −86.8‰ to −32.9‰ for δ^2H and −10.2‰ to 2.5‰ for δ^{18}O, and tended to cluster by both aquifer conditions and geographic location. In the Ejina Delta, the shallow, middle and deep groundwaters exhibited similar stable isotopic compositions, and the spring water was more depleted (Fig. 4). Additionally, the groundwater in the Gurinai and Guaizihu areas differed from the groundwater in the Ejina Delta in its isotopic pattern. The shallow groundwaters of the western and northern areas of the Badain Jaran Desert surrounding the Gurinai and Guaizihu areas exhibited a wide range of values for these parameters, particularly in δ^2H, which varied from −74.4‰ to −36.7‰.

5. Discussion

5.1. $\delta^{18}O/\delta^2H$ isotopes and groundwater provenance

A local meteoric water line (LMWL) for Zhangye (middle reaches of the Heihe Basin) provides the basis for the interpretation in this study. The isotope composition of precipitation and river water can be plotted along the LMWL (Fig. 4) using the equation δ^2H = 7.4δ^{18}O + 3.2 (Gates et al., 2008), which indicates its meteoric origin. The isotopic data from the lake water define a line with a regression equation of δ^2H = 4.8δ^{18}O − 15.2 (correlation coefficient: R^2 = 0.83), which intersects the LMWL at δ^2H = −49‰ and δ^{18}O = −7‰ (Fig. 4). This regression line can be interpreted as the local evaporation line (LEL) in the study area. The lake water samples are considered to be isotopically heavier than the groundwater due to strong evaporation. Additionally, the East Juyan Lake water was observed to become more enriched from June to September (from 2‰ to 33‰ for δ^2H, and from 2‰ to 13‰ for δ^{18}O) as a result of continual evaporation from the lake surface, and in late September, the lake water became depleted (−25.91‰ for δ^2H and −3.57‰ for δ^{18}O) when Heihe River water reached East Juyan Lake, as shown in Table 1.

As shown in Fig. 4, the isotopic composition of most shallow groundwater (exception to sampling sites No. 16, 18, 21–22) and partly deep groundwater (sampling sites No. 49, 51–53) in the Ejina Delta exhibits a narrow range, falling between −60‰ and −40‰ for δ^2H and between −8‰ and −5‰ for δ^{18}O, confirming that these groundwaters are expected to be characterized by the same general recharge source. Additionally, the isotope composition of these groundwaters mainly plots along the LMWL (Fig. 4), indicating their meteoric origin. However, it is noted that the spring water near East Juyan Lake (sampling sites No. 57 and 58) and the deep groundwater from the north of the Juyan Lakes (sampling sites No. 54 and 55) extremely depleted in both δ^{18}O (−11 to −8‰) and δ^2H (−86 to −76‰). This suggests that the deep groundwater in the confined aquifer must be of a paleo-water origin or a mixture of paleo-waters with modern waters (Chen et al., 2006). This conclusion is also confirmed by the interpretation of groundwater radiocarbon data, which indicated a residence time of 4000–9500 years for the deep confined groundwater (Su et al., 2009). In contrast, the isotope composition of the groundwater in the Gurinai and Guaizihu areas, as plotted in the δ^{18}O versus δ^2H diagram, shows a different pattern than the isotope composition in the Ejina Delta (Fig. 4). The groundwater from the Gurinai area is enriched to values between −7.1‰ and +2.5‰ δ^{18}O along a line with a slope of 3.0 that intercepts the LMWL at −10.5‰ δ^{18}O, and the isotopic data
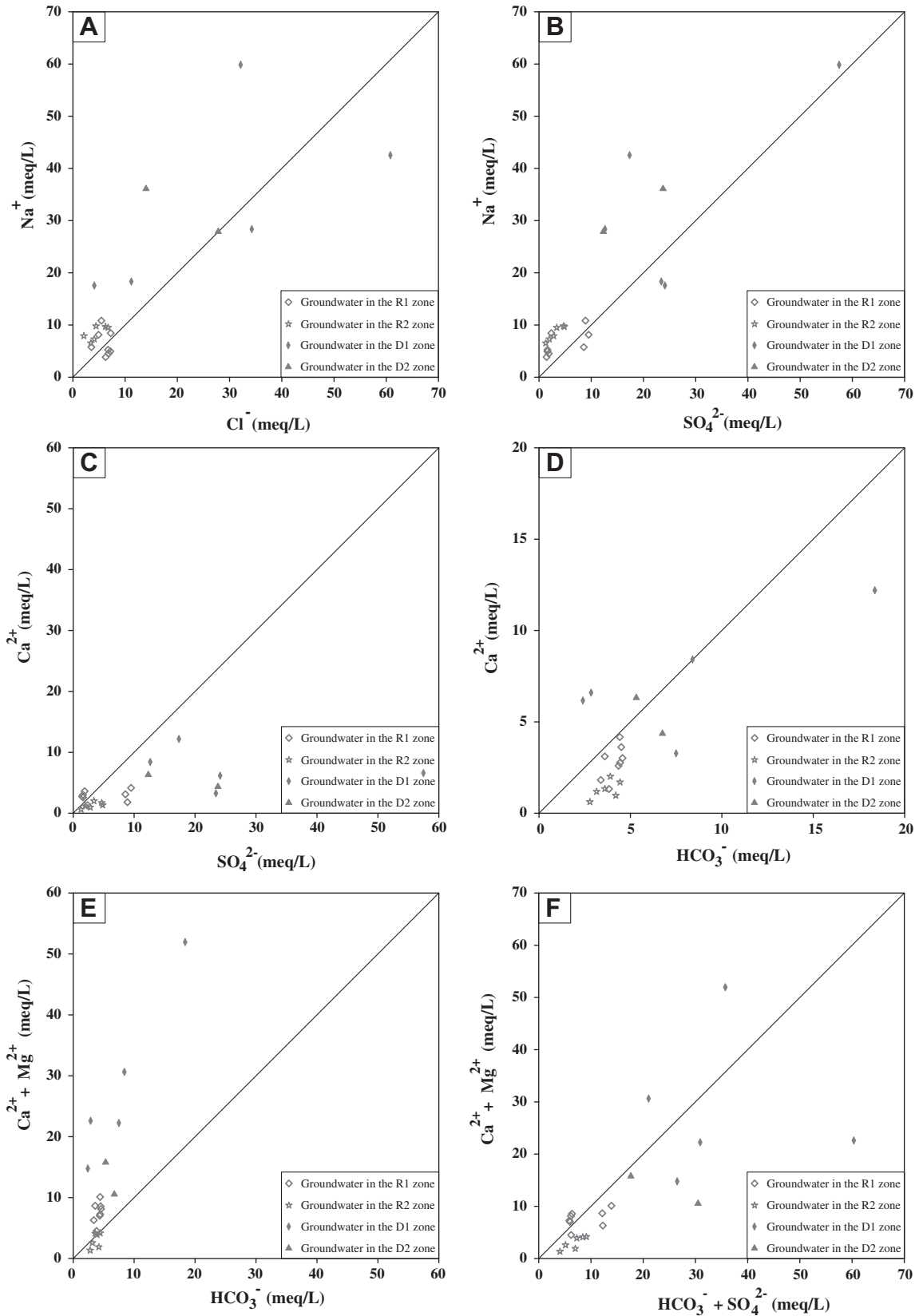
Fig. 8. Relation between various ions in the shallow phreatic groundwater.

of the Guaizihu groundwater is plotted along a line with a slope of 3.8 that intercepts the LMWL at −13‰ $\delta^{18}O$. The lower slope of the local evaporation lines, which is in the range of 3.0–4.0, suggests

the occurrence of strong evaporation processes in the pore water of the unsaturated zone below dry cover sediments (Geyh and Gu, 1999).
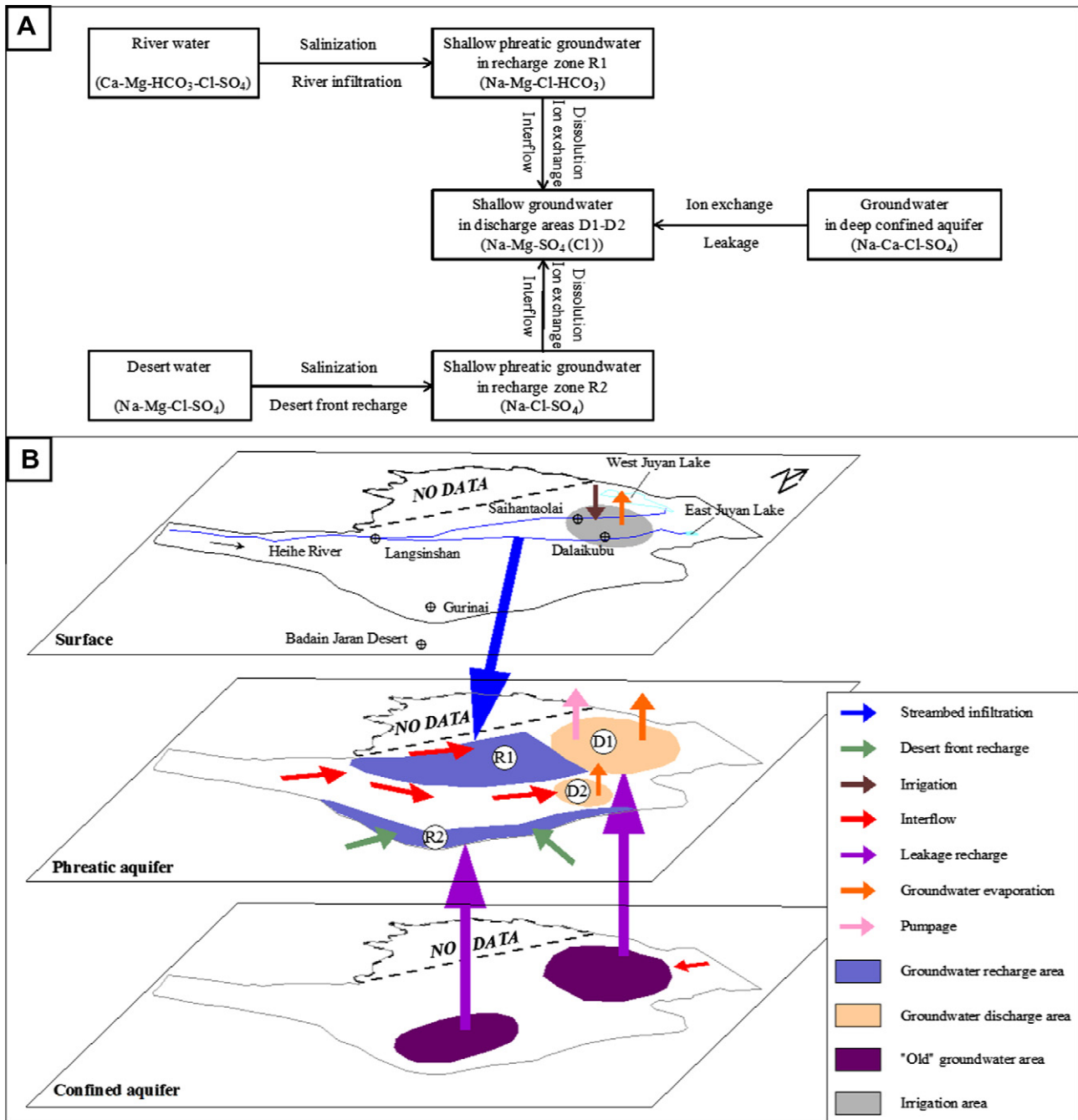
Fig. 9. Outline of mechanisms controlling the chemistry of surface and groundwater (up) and schema of the flow pattern (down) in the Ejina Basin.

The isotopic compositions of Badain Jaran Desert groundwater show the same pattern as the shallow groundwater from the bordering range of the Desert (the areas of Gurinai and Guaizihu) (Fig. 4). This suggests that the groundwater from Gurinai and the Badain Jaran Desert may be have the same recharge source, and the bordering range of the Badain Jaran Desert is a likely discharge zone of the desert water, as indicated by Gates et al. (2008). Additionally, data for the groundwater $\delta^{18}O–\delta^2H$ compositions from Badain Jaran Desert and the deep confined aquifer in the area of terminal lakes (sampling sites No. 50, 54, 57–58) plot almost along the same evaporation line (Table 1 and Fig. 4), implying the similar recharge source of the desert water and deep confined groundwater around the Juyan Lakes. Previous studies also indicated that the groundwater within the Desert was paleo-water recharged either

during the late Pleistocene or during wetter climatic periods within the Holocene (Yang et al., 2003, 2010; Edmunds et al., 2006; Ma and Edmunds, 2006) and that the deep confined groundwater in the Ejina Basin was formed in a colder and wetter climate during the late Pleistocene and Holocene (Chen et al., 2006; Zhu et al., 2008; Su et al., 2009).

5.2. Identification and spatial distribution of groundwater chemistry

The chemical composition of groundwater evolves during regional flows, and this evolution can be generalized by considering the water types that are typically found in different zones of groundwater flow systems (Ingebritsen et al., 2006). The Piper diagram (Piper, 1944) is a graphical representation of the chemistry of

water samples and is widely used to evaluate the hydrochemical evolution of surface water and groundwater (Subrahmanyam and Yadaiah, 2001). As shown in Fig. 5, it can be seen that almost all water samples fall into zone 4, indicating that the surface and groundwaters are dominated by SO_4 and Cl. The river water is of an HCO_3–Cl–SO_4 type, in which HCO_3 accounts for 55%, Cl 20–25%, and SO_4 20–25% of the total anions. The lake water appears to be dominated by SO_4–Cl, and the concentrations of the major cations are in the order of Na + K > Mg > Ca (Fig. 5A).

The groundwater samples are variable in their major ion compositions, though they are generally Na + K rich with no dominant anion type (Fig. 5B and C). The cation triangular diagram shows that the shallow phreatic groundwater chemistry is characterized by two groups. The first group is distributed in the bordering range of the Badain Jaran Desert (Gurinai and Guaizihu areas) and is characterized by Na type groundwater, in which Na accounts for >60% of the total anions. This water group is similar to the desert shallow groundwater with respect to the water type (Fig. 5B), and neither the total mineralization nor the major ion composition are clearly distinguishable between them, suggesting the discharge process from the Desert to the bordering areas. The second group is distributed in the Ejina Delta and is characterized by Na–Mg type or Mg–Na type groundwater, in which Na accounts for 30–70% and Mg 20–45% of the total anions (Table 1 and Fig. 5B). In addition, the shallow phreatic groundwater in the Ejina Delta could be grouped into a Cl–HCO_3 (or Cl) type within the river water influence zone (a front range of the Ejina Delta) and an SO_4 type in the rest of the area. The groundwater in the area of the East and West Juyan Lakes (a discharge sector of the groundwater system with a low elevation) has a different major ion composition than other areas, which is representative of the lack or the low rates of modern recharge. In this area, the shallow phreatic groundwater (Na–Mg–SO_4–Cl or Na–Mg–Cl–SO_4 type water) differs from the deep confined groundwater (Na–Ca–Cl–SO_4 type water) in water type; however, the deep confined groundwater is similar to the groundwater from the Desert and its bordering range with respect to the ionic composition (Na–Mg–Cl–SO_4 type water) (Table 1 and Fig. 5B and C), which indicates that groundwater in these areas could possibly be formed by the similar hydrochemical processes.

The shallow phreatic groundwater TDS exhibits notable spatial heterogeneity, varying from 0.365 g/L to 5.833 g/L. As shown in Fig. 6A, the freshwater zone (TDS < 1 g/L) of the shallow phreatic groundwater is mainly distributed in the front range of the Ejina Delta (zone R1) and the bordering range of the Badain Jaran Desert (zone R2 and R3), where there are improved recharge and cycling conditions. The groundwater in this zone belongs to the Na–Mg–Ca–Cl–HCO_3 or Na–Cl–SO_4 water types. The slightly saline water zone (TDS = 1–3 g/L) is mainly distributed between the Ejina Delta and the Badain Jaran Desert, and the groundwater chemistry in this area is characterized by the Na–Mg–SO_4 (Cl) water type. The saline water (TDS > 3 g/L) is distributed in the area of the East and West Juyan Lakes (zone D1), and it overlaps with the main accumulation of Quaternary sediments (Fig. 6A). The groundwater in this zone belongs to Na–Mg–Cl–SO_4 or Na–Cl–SO_4 water type. The variation of the shallow phreatic groundwater TDS and the major ions is mainly affected by recharge, runoff and discharge conditions and exhibits distinct horizontal zonation from the periphery towards to the area of East and West Juyan Lakes (Xie, 1980). Generally, the increasing TDS in the groundwater resulted from the occurrence of dissolving mineral in the direction of groundwater flow. In addition, the widespread exploitation of groundwater resources has exacerbated the process of salinization of groundwater in this region to some extent (Su et al., 2007, 2009; Guo et al., 2009).

During the study period, the salinity in the shallow phreatic groundwater varied from 1.2% to 14.4%, and a significant zonation

in salinity could be identified along the regional flow direction from the recharge area to the discharge area. As shown in Fig. 6B, the groundwater recharge zones with low-salinity (from 1% to 3.5%) are mainly distributed in the front range of the Ejina Delta (zone R1) and the bordering range of the Badain Jaran Desert (zone R2 and R3). Accumulation of salinity occurs in shallow phreatic groundwater during regional flows due to in situ reactions (Ingebritsen et al., 2006), and the high-salinity (more than 5%) was observed in the area of the East and West Juyan Lakes (zone D1), as well as the Northern Gurinai Depression (zone D2), which are the area most affected by evaporation. The higher than normal salinities in the northwestern Saihantaolai-Dalaikubu Depression are also considered to be the result of irrigation return flows (Wen et al., 2005).

A comparison of Figs. 3 and 6 shows that the shallow groundwater recharge areas of the Ejina Basin are dominant in the zones R1-R2 (zone R1 includes sampling sites No. 8–15; zone R2 includes sampling sites No. 24, 26–30), while the areas of shallow groundwater discharge occur mainly in the zones D1-D2 (zone D1 includes sampling sites No. 19–23; zone D2 includes sampling sites No. 33–34). Shallow phreatic groundwater in recharge and discharge areas may be distinguished from the relationship between TDS and total alkalinity concentrations: shallow groundwater in the recharge areas has the lower TDS values (<1000 mg/L), as well as the lower alkalinity concentrations (<5 meq/L); however, TDS values of shallow groundwater in the discharge areas is greater than 2000 mg/L, and total alkalinity concentrations vary from 2 meq/L to 20 meq/L.

5.3. Mechanisms controlling nature waters chemistry

The diagrams of the weight ratios between TDS and Na/(Na + Ca) (Gibbs, 1970) show that the major mechanisms controlling the nature waters chemistry could be defined as rock dominance and the evaporation–crystallization process (Fig. 7). The surface waters show an evolutionary path, illustrated by narrow in Fig. 7A, starting from near the Ca end-member with changes in composition toward the Na-rich, high-salinity end-member as the Heihe River flows toward the East Juyan Lake. This change in composition and concentration along the length of the Hehei River is due to evaporation, which increases salinity, as well as the relative proportion of Na to Ca (Gibbs, 1970). The high sodium concentration in the lake water (>940 mg/L) also indicates that evaporation is the prime factor controlling the surface water chemistry.

Referring to natural mechanisms that control the shallow phreatic groundwater chemistry, there is a significant difference between recharge and discharge areas. As shown in Fig. 7B, the chemical composition of groundwater in the recharge areas is controlled primarily by rock dominance, while the major mechanism that controlling the chemical composition of groundwater in the discharge areas is the evaporation-fractional crystallization process. Moreover, it is noted that the weight ratio Na/(Na + Ca) of groundwater in the zone R2 (0.8–1.0) is higher than in the zone R1 (0.6–0.8), indicating additional mechanisms that contribute to the exact composition of groundwater in the zone R2. A presentation of the major cations and total salinity for deep confined groundwater (Fig. 7C) is similar to that for the shallow phreatic groundwater in recharge areas. This presentation again defines the major mechanism controlling the deep confined groundwater chemistry as rock dominance such as interactions between water and the dominant rock.

Dissolved species and their compositional relations can reveal the origin of solutes and the hydrochemical processes that generated the observed water compositions such as simple mixing, ion exchange and chemical reactions (Fisher and Mullican, 1997; Hiscock, 2005). The positive relationships observed between Na

with Cl (R = 0.81) in the study area indicate that major ionic composition (Na and Cl) is mainly derived from halite dissolution (Zhu et al., 2008; Su et al., 2009); however, the excess of Na over Cl at low chloride concentrations for most groundwater samples from the recharge areas (Fig. 8A) is typically interpreted as reflecting Na released from the weathering of Na- and K- rich minerals or from the secondary processes, such as Ca/Na(K) ion exchange (Edmunds et al., 2003; Appelo and Postma, 2006). A scatter plot of Na versus SO_4 shows the increase in alkalis corresponds to a simultaneous increase in SO_4 (Fig. 8B), thereby indicating another potential source of excess Na may be from dissolving sodium sulfate (Na_2SO_4). Ca and SO_4 exhibit a good correlation, suggesting that dissolution of gypsum ($CaSO_4 \cdot 2H_2O$) possibly exerts a dominant control on the Ca chemistry; however, there is too little Ca relative to SO_4 for gypsum alone to be responsible for Ca chemistry (Fig. 8C). Good correlations between Ca and HCO_3 from recharge areas (Fig. 8D) suggest that weathering of calcite ($CaCO_3$) and dolomite ($CaMg(CO_3)_2$) also contributes Ca ions to the shallow phreatic groundwater. The plot of (Ca + Mg) versus HCO_3 (Fig. 8E) shows that most of the sample points lie above the equiline (1:1) and only a few points are below this line. This suggests that the excess of alkaline earth elements (Ca + Mg) over HCO_3 has been balanced by Cl and SO_4. In the study area, Ca, Mg, SO_4 and HCO_3 are mainly derived from simple dissolution of calcite, dolomite, and gypsum (Su et al., 2009), and a charge balance should exist between the cations and anion. However, a deficiency of (Ca + Mg) relative to (SO_4 + HCO_3) exists in shallow phreatic groundwater, as indicated in the plot in Fig. 8F. Therefore, the excess negative charge of SO_4 and HCO_3 must be balanced by Na, and suggest that dissolution of trona ($Na_2CO_3 \cdot NaHCO_3 \cdot 2H_2O$) may be controlling the sodium and bicarbonate (Ma et al., 2009).

Geochemical processes that may be responsible for the various groundwater types are illustrated in Fig. 9A. During recharge (riverbank infiltration or irrigation return flows), evaporation concentrates the phreatic groundwater and leads to precipitation and the deposition of evaporites that are eventually leached into the saturated zone (Su et al., 2009). Additionally, the mixing of environmental flows with groundwater could also lead to a controlling influence on water chemistry. The groundwater in the recharge zone R1 (Na–Mg–Cl–HCO_3) is generally fresh as a result of periodic mixing with weakly mineralized river water (Ca–Mg–HCO_3–Cl) during periods of environmental flow controls in the Heihe River (Fig. 9A). Our results confirm that there is a trend towards evaporation in the Juyan Lakes region and that rock-dominated weathering is associated with the river water influence zone (Su et al., 2009). The formation of Na–Cl–SO_4 water in the recharge zone R2 is primarily a result of progressive salinization of the desert water (Na–Mg–Cl–SO_4) during the desert front recharge. Groundwater salinization in this zone would be expected to result from the ionic concentrations increasing due to both the evaporation of recharge water and to the effects of interactions between the groundwater and geological formations. Water composition evolves from mixed in recharge areas to Na–Mg–SO_4 (Cl) water types at the end of flow path with high concentration of alkalinity (zones D1–D2). A number of studies (Wen et al., 2005; Zhu et al., 2008; Si et al., 2009) showed that the groundwater in the study area was generally undersaturated (SI: saturation index <0) with respect to sulfate phases and was near saturation with respect to calcite and dolomite. Thus, the changes in groundwater composition within the discharge areas are consistent with dissolution of sulfate minerals and cation exchange. The existence of soluble-salt deposits within a local aquifer system (Xie, 1980) as well as rock-water interactions plays a dominant role in determining the water type in the deep confined aquifer (Na–Ca–Cl–SO_4). The dissolution of bedded halite leads to large increases in sodium and chloride. The confined groundwater can also have a profound effect on

phreatic groundwater chemistry as a result of the process of mixing between them.

5.4. Recharge mechanism and a conceptual model of groundwater flow

Based on the new hydrochemical and isotopic data and supported by the earlier studies, we propose a conceptual model of recharge to the Ejina Basin, exception to the west region (Fig. 9B). Runoff generated from Qilian Mountain is the main source of surface water and groundwater for the Heihe Basin, which ultimately reaches the East and West Juyan Lakes (Jin et al., 2008). By the 1960s, surface and groundwater were abundant in the Ejina Basin (Wu et al., 2002), and the shallow aquifer was replenished by direct infiltration from the Heihe River. From 1960 onwards, with the decrease in the surface water from the Heihe River as a result of increased irrigation in its middle reaches, the West and East Juyan Lakes became dry in 1961 and 1992, respectively (Jin et al., 2008). Due to changes in surface hydrological processes and groundwater exploitation, the shallow groundwater level in the Ejina Basin has markedly dropped in the last decades (Su et al., 2007). Recently, the regional decline of the groundwater level in the whole basin has continued to occur; however, the local groundwater level has been rising for approximately 10 years due to environmental flow controls aimed at delivering a set amount of surface water to East Juyan Lake and the Ejina Oasis (Wang et al., 2011a). The stable isotope signatures from the shallow groundwater in the front range of the Ejina Delta illustrate its close connection with the surface water. The local evaporation line also confirms that the shallow groundwater is recharged by surface water, and additional evaporation from the surface water is demonstrated by further enrichment along the evaporation line.

Direct infiltration from the Heihe River remains the main source of shallow groundwater, while the surface water recharge is insufficient to support the current shallow groundwater levels. An additional recharge to the Ejina aquifer may be originated from the Badain Jaran Desert (Qian et al., 2006). The isotopic compositions of the shallow groundwater samples from the areas of Gurinai (west of the Desert) and Guaizihu (north of the Desert) tend to conform to the same pattern as the groundwater samples from the Desert. They evolved from meteoric water similar to the Badain Jaran samples and have been similarly enriched by evaporation. Moreover, the range of isotopic values for the spring water is the same as that of the groundwater in the Badain Jaran Desert, and this is in accord with the evaporation line, indicating the same recharge source. Gurinai and Guaizihu are most likely a discharge zone for the Badain Jaran shallow aquifer, considering regional hydraulic head patterns (Gates et al., 2008). At present, the Gurinai wetland has almost disappeared because the desert groundwater did not effuse with the decrease of the water quantity, though it is still recharging the small lakes through spring water in the bordering range of the Desert. The hypothesis of springs coming from deeper formations as a source of the desert margin shallow groundwater is inconsistent with the Cl concentrations in the Badain Jaran shallow groundwaters, which are lower than in most deep groundwater samples (Gates et al., 2008).

The other potential recharge sources for the deep confined aquifer in the area of Juyan Lakes are the "old" groundwaters from the north Mongolia plateau (Zhang et al., 2005; Qian et al., 2006), which is consistent with the results of groundwater flow modeling analysis (Xi et al., 2010a). Furthermore, deep confined groundwater is connected to the shallow aquifer system within the Ejina Basin, and the direct recharge of shallow groundwater comes from the vertical leakage from the lower confined aquifer. Evidence of deep groundwater recharge is present in the spring water in the area of the East and West Juyan Lakes.

According to the determined isotopic and hydrochemical characteristics, the groundwater samples could be divided into three areas: a front range of the Ejina Delta, an area bordering the Badain Jaran Desert (Gurinai and Guaizihu areas), and an area of the Juyan Lakes and the Gurinai Depression. By analyzing the spatial distribution of the shallow groundwater TDS and salinity, the front range of the Ejina Delta and the bordering range of the Desert are considered to be recharge areas, and the area of the Juyan Lakes and Gurinai Depression are discharge areas. Accordingly, three main recharge mechanisms for the Ejina aquifer are possible: river infiltration, desert front recharge and lateral/vertical groundwater flow. Under natural conditions, evapotranspiration is the main route of the regional groundwater discharge. Evapotranspiration of groundwater in the shallow phreatic aquifer mainly occurred in the northern part of the basin and the Gurinai area. Groundwater flows from recharge areas toward discharge areas and then is lost to evaporation. The other output sources are evaporation from the lake, surface and groundwater flows, and local groundwater extraction for irrigation, industry and domestic use.

6. Conclusions

The sources and recharge mechanisms of the groundwater in the Ejina Basin were considered on the basis of isotopic and hydrochemical analysis. This comprehensive analysis led to the identification of modern groundwater recharge to the Ejina Basin from the Heihe River. Another important recharge source is groundwater from the Badain Jaran Desert aquifer, which was formed in a colder and wetter climate during the late Pleistocene and Holocene. Based on the spatial distribution of the hydrochemical constituents of the shallow groundwater, the front range of the Ejina Delta and the bordering range of the Badain Jaran Desert, where there are improved cycling conditions and distributed freshwater, could be considered as recharge zones. Discharge zones of regional flows are confirmed as existing in the East and West Juyan Lakes, as well as in the Northern Gurinai Depression, where there is accelerated salt accumulation in the groundwater as a result of strong evaporation. The major ion chemistry accumulates continuously along the shallow groundwater flow paths, and evolves from a dilute calcium bicarbonate type in the recharge areas toward a more concentrated sodium chloride or calcium chloride type in the discharge areas. The buildup of dissolved solids through evaporation represents a major controlling mechanism of the groundwater composition, and the dominant anion species change systematically from HCO_3 to SO_4 to Cl; however, the dissolved ions from sulfate minerals and bedded halite also contribute significantly.

Based on our analyses of hydrochemical characteristics and isotopic tracers, river infiltration, desert front recharge and lateral/vertical groundwater flows could be considered as the three main recharge mechanisms for the Ejina aquifer. Evaporation from the lake, surface and groundwater flows, and groundwater extraction for irrigation represent the mechanisms of discharge processes in the study area. The cycling between surface water and shallow groundwater during periods of environmental flow controls suggests that the surface/groundwater interaction is the dominant recharge process in the study area. Based on observations of the depression springs in the Gurinai and Guaizihu areas, desert front recharge to the Ejina Basin is still occurring; however, the disappearance of lakes that formerly existed in these areas indicates that the groundwater recharge rate from the Badain Jaran Desert aquifer has significantly decreased. Therefore, the improvement of groundwater quality and quantity in this ecologically sensitive area must be based on shallow groundwater recharge of the phreatic aquifer in the Ejina Delta, which mainly takes place via seepage through the riverbed and direct infiltration during periods of environmental flow controls.

References

Akiyama, T., Sakai, A., Yamazaki, Y., Wang, G., Fujita, K., Nakawo, M., Masayoshi, A., Jurhpei, A., Yuki, G., 2007. Surface water–groundwater interaction in the Heihe River basin, Northwestern China. Bull. Glaciol. Res. 24, 87–94.

Appelo, C.A.J., Postma, D., 2006. Geochemistry, Groundwater and Pollution, second ed. A.A. Balkema Publishers, Leiden, The Netherlands.

Chen, F., Wu, W., Holmes, J.A., Madsen, D.B., Zhu, Y., Jin, M., Oviatt, C.G., 2003. A mid-Holocene drought interval as evidenced by lake desiccation in the Alashan Plateau, Inner Mongolia, China. Chin. Sci. Bull. 48 (14), 1401–1410.

Chen, J., Wang, J., Zhao, X., Sheng, X., Gu, W., Chen, L., Su, Z., 2004a. Study of groundwater supply of the confined Aquifers in the Ejina Basin based on isotopic methods. Geol. Rev. 50 (6), 649–658 (in Chinese with English abstract).

Chen, Z., Nie, Z., Zhang, H., Cheng, X., He, M., 2004b. Groundwater renewability based on groundwater ages in the Heihe valley alluvial basin, Northwestern China. Acta Geol. Sinica 4, 560–567 (in Chinese with English abstract).

Chen, Y., Zhang, D., Sun, Y., Liu, X., Wang, N., Savenije, H.H.G., 2005. Water demand management: a case study of the Heihe River Basin in China. Phys. Chem. Earth, Parts A/B/C 30 (6–7), 408–419.

Chen, Z., Nie, Z., Zhang, G., Wan, L., Shen, J., 2006. Environmental isotopic study on the recharge and residence time of groundwater in the Heihe River Basin, northwestern China. Hydrogeol. J. 14 (8), 1635–1651.

Edmunds, W.M., Guendouz, A.H., Mamou, A., Moulla, A., Shand, P., Zouari, K., 2003. Groundwater evolution in the Continental Intercalaire aquifer of southern Algeria and Tunisia: trace element and isotopic indicators. Appl. Geochem. 18 (6), 805–822.

Edmunds, W.M., Ma, J., Aeschbach-Hertig, W., Kipfer, R., Darbyshire, D.P.F., 2006. Groundwater recharge history and hydrogeochemical evolution in the Minqin Basin, North West China. Appl. Geochem. 21 (12), 2148–2170.

Feng, Q., Cheng, G., 1998. Current situation, problems and rational utilization of water resources in arid north-western China. J. Arid Environ. 40 (4), 373–382.

Feng, Q., Cheng, G.D., Endo, K.N., 2001. Towards sustainable development of the environmentally degraded River Heihe basin, China. Hydrol. Sci. J. 46 (5), 647–658.

Feng, Q., Liu, W., Su, Y.H., Zhang, Y.W., Si, J.H., 2004. Distribution and evolution of water chemistry in Heihe River basin. Environ. Geol. 45 (7), 947–956.

Fisher, R.S., Mullican, W.F., 1997. Hydrochemical evolution of sodium-sulfate and sodium-chloride groundwater beneath the Northern Chihuahuan Desert, Trans-Pecos, Texas, USA. Hydrogeol. J. 5 (2), 4–16.

Gates, J.B., Edmunds, W.M., Darling, W.G., Ma, J., Pang, Z., Young, A.A., 2008. Conceptual model of recharge to southeastern Badain Jaran Desert groundwater and lakes from environmental tracers. Appl. Geochem. 23 (12), 3519–3534.

Geyh, M.A., Gu, W.Z., 1999. Highly isotopically enriched shallow groundwater below overlying dry sediments. In: Isotope Techniques in Water Resources Development and Management 1999, IAEA.

Gibbs, R.J., 1970. Mechanisms controlling world water chemistry. Science 170, 1088–1090.

Guo, Q., Feng, Q., Li, J., 2009. Environmental changes after ecological water conveyance in the lower reaches of Heihe River, northwest China. Environ. Geol. 58 (7), 1387–1396.

Hiscock, K.M., 2005. Hydrogeology. Principles and Practice. Blackwell Publishing, Oxford, UK.

Ingebritsen, S.E., Sanford, W.E., Neuzil, C.E., 2006. Groundwater in Geologic Processes, second ed. Cambridge University Press.

Jin, X., Hu, G., Li, W., 2008. Hysteresis effect of runoff of the Heihe River on vegetation cover in the Ejina Oasis in Northwestern China. Earth Sci. Front. 15 (4), 198–203.

Ma, J., Edmunds, W., 2006. Groundwater and lake evolution in the Badain Jaran Desert ecosystem, Inner Mongolia. Hydrogeol. J. 14 (7), 1231–1243.

Ma, J., Ding, Z., Edmunds, W.M., Gates, J.B., Huang, T., 2009. Limits to recharge of groundwater from Tibetan plateau to the Gobi desert, implications for water management in the mountain front. J. Hydrol. 364 (1–2), 128–141.

Piper, A.M., 1944. A graphic procedure in the geochemical interpretations of water analyses. Trans. Am. Geophys. Union 25, 914–923.

Qian, Y., Qin, D., Pang, Z., Wang, L., 2006. A discussion of recharge sources of deep groundwater in the Ejin Basin in the lower reaches of Heihe River. Hydrogeol. Eng. Geol. 3, 25–29 (in Chinese with English abstract).

Si, J., Feng, Q., Wen, X., Su, Y., Xi, H., Chang, Z., 2009. Major ion chemistry of groundwater in the extreme arid region northwest China. Environ. Geol. 57 (5), 1079–1087.

Su, Y., Feng, Q., Zhu, G., Si, J., Zhang, Y., 2007. Identification and evolution of groundwater chemistry in the Ejin Sub-Basin of the Heihe River, Northwest China. Pedosphere 17 (3), 331–342.

Su, Y., Zhu, G., Feng, Q., Li, Z., Zhang, F., 2009. Environmental isotopic and hydrochemical study of groundwater in the Ejina Basin, northwest China. Environ. Geol. 58 (3), 601–614.

Subrahmanyam, K., Yadaiah, P., 2001. Assessment of the impact of industrial effluents on water quality in Patancheru and environs, Medak district, Andhra Pradesh, India. Hydrogeol. J. 9 (3), 297–312.

Wang, G., Cheng, G., 2000. The characteristics of water resources and the changes of the hydrological process and environment in the arid zone of northwest China. Environ. Geol. 39 (7), 783–790.

Wang, G., Yang, L., Chen, L., Jumpei, K., 2005. Impacts of land use changes on groundwater resources in the Heihe River Basin. J. Geog. Sci. 15 (4), 405–414.

Wang, X., Chen, F., Hasi, E., Li, J., 2008. Desertification in China: an assessment. Earth Sci. Rev. 88 (3–4), 188–206.

Wang, P., Yu, J., Zhang, Y., Fu, G., Min, L., Ao, F., 2011a. Impacts of environmental flow controls on the water table and groundwater chemistry in the Ejina Delta, northwestern China. Environ. Earth Sci. 64 (1), 15–24.

Wang, P., Zhang, Y., Yu, J., Fu, G., Ao, F., 2011b. Vegetation dynamics induced by groundwater fluctuations in the lower Heihe River Basin, northwestern China. J. Plant Ecol. 4 (1–2), 77–90.

Wen, X., Wu, Y., Su, J., Zhang, Y., Liu, F., 2005. Hydrochemical characteristics and salinity of groundwater in the Ejina Basin, Northwestern China. Environ. Geol. 48 (6), 665–675.

Wu, X., Shi, S., Li, Z., Hao, A., Qiao, W., Yu, Z., Zhang, S., 2002. The study on the groundwater flow system of Ejina basin in lower reaches of the Heihe River in Northwest China (Part 1). Hydrogeol. Eng. Geol. 1, 16–20 (in Chinese with English abstract).

Xi, H., Feng, Q., Liu, W., Si, J., Chang, Z., Su, Y., 2010a. The research of groundwater flow model in Ejina Basin, Northwestern China. Environ. Earth Sci. 60 (5), 953–963.

Xi, H., Feng, Q., Si, J., Chang, Z., Cao, S., 2010b. Impacts of river recharge on groundwater level and hydrochemistry in the lower reaches of Heihe River Watershed, northwestern China. Hydrogeol. J. 8, 791–801.

Xie, Q., 1980. Regional hydrogeological survey report of the People's Republic of China (1:200 000): Ejina K-47-[24] [R], Jiuquan (in Chinese).

Yang, X., Williams, M.A.J., 2003. The ion chemistry of lakes and late Holocene desiccation in the Badain Jaran Desert, Inner Mongolia, China. CATENA 51 (1), 45–60.

Yang, X., Liu, T., Xiao, H., 2003. Evolution of megadunes and lakes in the Badain Jaran Desert, Inner Mongolia, China during the last 31,000 years. Quatern. Int. 104 (1), 99–112.

Yang, X., Ma, N., Dong, J., Zhu, B., Xu, B., Ma, Z., Liu, J., 2010. Recharge to the inter-dune lakes and Holocene climatic changes in the Badain Jaran Desert, western China. Quatern. Res. 73 (1), 10–19.

Zhang, Y., Wu, Y., Su, J., Wen, X., Liu, F., 2005. Groundwater replenishment analysis by using natural isotopes in Ejina Basin, Northwestern China. Environ. Geol. 48 (1), 6–14.

Zhang, K., Wang, R., Han, H., Wang, X., Si, J., 2007. Hydrological and water resources effects under climate change in Heihe River Basin. Resour. Sci. 29 (1), 77–83 (in Chinese with English abstract).

Zhu, Y., Wu, Y., 2004. A survey: obstacles and strategies for the development of ground-water resources in arid inland river basins of Western China. J. Arid Environ. 59 (2), 351–367.

Zhu, G., Su, Y., Feng, Q., 2008. The hydrochemical characteristics and evolution of groundwater and surface water in the Heihe River Basin, northwest China. Hydrogeol. J. 16 (1), 167–182.

Zhu, Y., Ren, L., Skaggs, T.H., Lü, H., Yu, Z., Wu, Y., Fang, X., 2009. Simulation of *Populus euphratica* root uptake of groundwater in an arid woodland of the Ejina Basin, China. Hydrol. Process. 23 (17), 2460–2469.